The Design of Multimedia Multicasting Services in LTE HetNets Using Stochastic Geometry

Dragan Rastovac*, Dejan Vukobratovic*, Chadi Khirallah†, John Thompson†
*Dept. of Power, Electronics and Communication Engineering, University of Novi Sad, Serbia
†School of Engineering, The University of Edinburgh, Edinburgh, UK

***Abstract*—The mobile multimedia delivery services will continue to grow and dominate the traffic in upcoming 4G/5G cellular networks. 3GPP evolved Multimedia Multicast/Broadcast Service (eMBMS) will require considerable service resources for high-quality video delivery with high coverage probability. In this paper, we consider a simple approach to estimate achievable rates and optimally assign the physical layer transmission parameters for eMBMS based video service in the two-tier heterogeneous cellular systems. We use stochastic geometry based analysis recently investigated in the literature to obtain coverage probabilities for different power and density ratios among the base station tiers. As a result, we are able to derive average area throughput and design the optimized LTE/LTE-A HetNets configurations for improved eMBMS service delivery.**

I. Introduction

Recent estimates predict increase in the wireless Internet traffic over the fourth generation (4G) cellular networks that can be attributed mainly to multimedia delivery services. Cisco Visual Networking Index estimate that the mobile multimedia traffic will increase 13-fold in the period 2012-2017. For example, by 2013, the Internet video will account for over 50% of the total Internet traffic, whereas by 2015, the mobile multimedia traffic will account for 66.4% of all mobile data traffic [1]. The evolving 3GPP Long Term Evolution (LTE) and LTE-Advanced (LTE-A) cellular standards represent a response of industry and standardization to ever increasing mobile traffic [2]. In this work, we focus on the mobile video multicasting/broadcasting services provided by the 3GPP evolved Multimedia Multicast/Broadcast Service (eMBMS) [3]. The eMBMS is recently enhanced service solution with two proposed transmission schemes: the single frequency network eMBMS (SFN-eMBMS) and a single-cell eMBMS (SCeMBMS)[4] optimized for large-scale content multicasting over cellular infrastructure.

Mathematical analysis of the conventional hexagonal grid-model cellular networks, extensively used both in industry and academia over the past three decades, is known to be hard. The signal to interference and noise (SINR) expressions resulting from such a model are complex and metrics of interest are usually estimated by Monte Carlo methods or simplified and potentially inaccurate Wyner model [5]. Modern cellular networks are becoming even more complex due to the deployment of multiple tiers of base stations (eNB) that have different characteristics. However, for some reasonably simple and sufficiently accurate spatial deployment models such as the distributions of base station tiers following Poisson point process (PPP), the resulting SINR coverage analysis using stochastic geometry tools yields surprisingly simple closed-form expressions [6][7].

In this paper, due to its analytical appeal, we apply stochastic geometry results for PPP base station placement models to analyse eMBMS video delivery over LTE-A HetNets. We investigate achievable rates and coverage for eMBMS based video service delivery in LTE-A HetNets modelled as the two-tier cellular systems. We apply realistic simulation results that employ 3GPP-defined channel models to *calibrate* the parametrized stochastic geometry based coverage probability evaluation. Then, a simple and calibrated coverage probability equations are applied to investigate achievable rates and coverage in various two-tier LTE-A HetNets configurations.

The rest of the paper is organized as follows. Sec. II provides necessary background. In Sec. III, we present the system model and methodology for evaluation of average service data rates at mobile devices (UE) serviced within the cell. The same section includes 3GPP and stochastic geometry models of different eNB classes. Simulation results achievable rates for eMBMS service are presented in Sec. IV. The paper is concluded in Sec. V.

II. Background

A. Video Multicasting Services Over LTE/LTE-A

3GPP standards for mobile multimedia delivery over cellular networks defines MBMS as a suitable platform for multicasting the same video content to a large number of users over a common radio channel [3]. 3GPP standards present architectural design for MBMS point-to-multipoint transmission schemes starting from Release 6 [4]. The enhanced version of MBMS, called eMBMS, is introduced by providing two transmission options in Release 8 [8]. The first one, named single-cell (SC-eMBMS) transmission, allows user feedback on channel conditions and adaptive selection of the modulation and coding (MC) schemes at the physical layer. The advantage of this scheme is dynamic adaptation to current profile of users in the cell. Furthermore, in terms of energy efficiency, the SC-eMBMS service can be switched-off in the cells with no active service. The second one, single frequency network (SFN-eMBMS) transmission, represents a coordinated effort of macro eNBs to cover the network with the same physical signal, with MC scheme adapted to the worst-case user requirements. SFN-eMBMS results in increased achievable

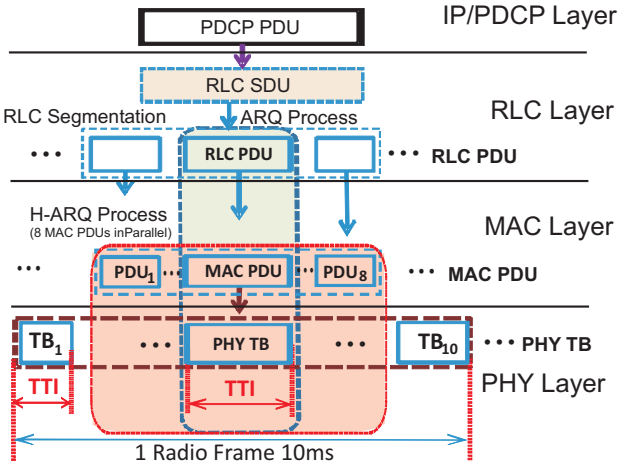

Fig. 1. eNB DL packet flow from IP to PHY layer.

rates at the cell edge [9] and does not depend on the user's distribution over the cell [4].

B. 3GPP LTE/LTE-A RAN Protocols

Video content is delivered through IP packet flows from eNB to the mobile UE via E-UTRAN radio-link connections [10]. The set of protocol responsible for IP flow downlink delivery at the eNB/UE interface, illustrated Fig. 1. Following Packet Data Conversion Protocol (PDCP), PDCP encapsulated IP packets (IP/PDCP) are delivered to the Radio Link Control (RLC) layer. The RLC layer segments/concatenates IP/PDCP packets into RLC packets to exactly match the MAC frame size requirements. The MAC frame size is dynamically provided by the MAC Scheduler to fit the upcoming PHY transport block (TB) size. PHY TB size depends on the MC scheme applied at the eNB, which in turn depend on the channel conditions reported by UEs [11].

Besides the MC scheme selected by the MAC Scheduler, the PHY TB size (TBS) within a single transmission time interval (TTI) depends on the amount of frequency resources: PHY resource blocks (RBs) allocated to the service delivery. The PHY RB represents a unit of time-frequency resources: 0.5 ms time duration ($\frac{1}{2}$ TTI) and 12 OFDM carriers (180 kHz) of bandwidth. PHY RBs are always allocated in pairs, thus the PHY TBS depends on the number N_{RBP} of RB pairs (RBPs), 1 RBP = 180 kHz $\times$ 1 TTI (see Table I in [12], for CQI states $3-15$ and CQI states $1-3$ calculation from Table 7.2.3-1 [13], TBS column for the case $N_{RBP}=6$, i.e., a Category 1 LTE user).

For SC-eMBMS, PHY TB size can be changed dynamically based on the UE feedback in the form of Channel Quality Indicator (CQI) values. In contrast, SFN-eMBMS is fixed in advance and does not allow dynamic changes of MC scheme. For more details on the LTE E-UTRAN protocols, we refer the reader to [11] [14].

III. The System Model

We consider multicast service delivery over the LTE/LTE-A HetNets modelled as multi-tier cellular system. We assume macro and pico eNBs are randomly placed according to Poisson point processes Φ_m and Φ_p of densities λ_m and λ_p, and transmit powers P_m and P_p, respectively. Each class of eNBs (macro and pico) is allocated a separate and disjoint set of PHY RBs (the same approach can be used if small cells reuse the same set of PHY RBs as the macro-cellular network). We assume a UE connects to the strongest candidate BS irrespective of the tier it belongs to.

We are interested in the coverage probability $P_c = \mathbb{P}(SINR(x) \geq \beta)$ where β is a given SINR threshold and $SINR(x)$ is SINR of a user uniformly and randomly placed in the area under consideration. As noted earlier, for the observed two-tier deployment model, we can get coverage SINR statistics in two ways: i) using equations derived from stochastic geometry, and ii) by employing realistic 3GPP models using simulations. We apply stochastic geometry equations for their simplicity, but also, apply simulated 3GPP models in order to accurately parametrize stochastic geometry equations.

A. Stochastic Geometry Model

We observe LTE-A HetNets represented as a K-tier cellular network model [15] and each of K tiers models different class of the BSs. The BSs across tiers may differ in terms of transmit power and spatial density. We assume a UE to be in coverage if it is able to connect to at least one BS at any tier with SINR above a given threshold. In the case when all the tiers have the same SINR threshold β, coverage probability is precisely the complementary cumulative distribution function (CCDF) of the effective received SINR. Autors in [15] conduct analysis on a UE located at the origin. The fading between a BS located at point x and the UE is denoted by h_x and is assumed to be Rayleigh fading. Path loss function is given by $l(x) = \|x\|^{-\alpha}$, where $\alpha > 2$ is the path loss exponent. Hence, the received power at UE from a BS located at point x_i (belonging to the i-th tier) is $P_i h_{x_i} \|x_i\|^{-\alpha}$, where $h_{x_i} \approx exp(1)$. The average SINR at the UE is [15]:

$$SINR(x_i) = \frac{P_i h_{x_i} \|x_i\|^{-\alpha}}{\sum_{j=1}^{K} \sum_{x \in \Phi_i / x_i} P_j h_x \|x_i\|^{-\alpha} + \sigma^2}, \quad (1)$$

where σ^2 is the constant additive noise power.

We assume the open access strategy (discussed in [15]) where a UE is allowed to connect to any tier without any restrictions. The coverage probability P_c in open access network model is given by (Th.1 and Corollary 1, Sec. IIIA, [15]):

$$P_c(\{\lambda_i\}, \{\beta_i\}, \{P_i\}) = \frac{\pi}{C(\alpha)} \frac{\sum_{i=1}^{K} \lambda_i P_i^{2/\alpha} \beta_i^{-2/\alpha}}{\sum_{i=1}^{K} \lambda_i P_i^{2/\alpha}}, \quad (2)$$

where is $\beta_i > 1$. For $K = 1$ (1-tier network) the coverage probability is given by:

$$P_c(\lambda, \beta, P) = \frac{\pi}{C(\alpha) \beta^{2/\alpha}} \quad (3)$$

In (3), it is noted that P_c in 1-tier network is interference-limited and independent of the density of BSs, and solely dependent upon the target signal to interference ratio (SIR). This is consistent with [16], where a similar observation was

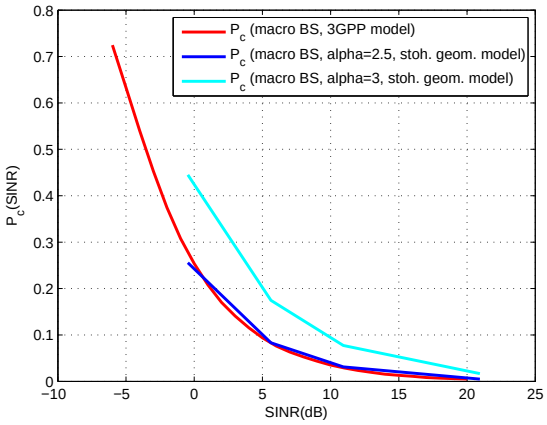

Fig. 2. Matching P_c 3GPP and the stochastic geometry model 1-tier networks (only macro BS).

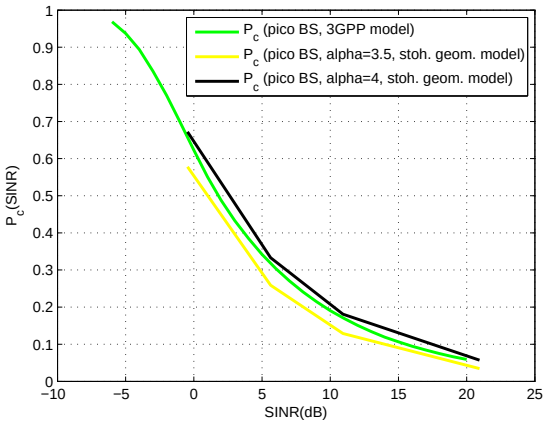

Fig. 3. Matching P_c 3GPP and the stochastic geometry model 1-tier networks (only pico BS).

made for a 1-tier network using nearest neighbour connectivity model [15]. In the following, we compare the P_c expression obtained by the stochastic geometry model (for 1-tier and 2-tier) with the simulation results using realistic 3GPP channel models. The goal is to fine-tune the path loss α parameter in the stochastic geometry model to match a realistic 3GPP model, and thereafter, to use simple stochastic geometry based analytical expressions for P_c.

B. 3GPP-Defined Model

In contrast to the previous model, we apply 3GPP defined path loss models and use simulations to evaluate coverage probabilities. For a path loss model, if a UE placed at a distance d from the eNB, the average SINR at the UE is obtained as [17]:

$$SINR(d) = P_{TX} + G_{TX} + G_{RX} - \\ -N - I - S(d) - PL(d) - PNL, \quad (4)$$

where P_{TX} is the eNB transmission power; G_{TX} and G_{RX} are the eNB and the UE antenna gains (including 3GPP defined horizontal and vertical antenna patterns for macro eNBs); N and I are the noise and the inter cell interference (ICI) power from all the interfering eNBs at the UE location; PNL is the wall penetration loss for signals received at indoor UEs; and finally, S and PL are the shadowing loss and the pathloss in dB measured at different UE positions using shadowing variances and path loss models defined in [17]. In the simulated model, BSs of different tiers are distributed according to PPP over the area of interest (e.g., unit square). Then, a sufficiently fine square-grid of UE positions is overlaid, and for each grid point, we calculate received SINR using the same rules as in stochastic geometry model. Finally, the coverage probability P_c is estimated as a fraction of grid points that exceeds a given SINR threshold β (averaged over a large number of BS deployments).

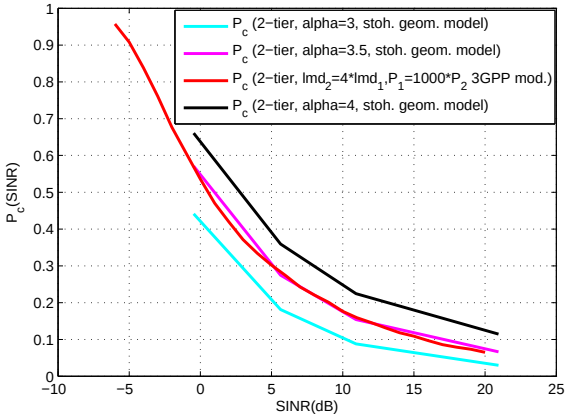

Fig. 4. Matching P_c 3GPP and the stochastic geometry model 2-tier networks (macro+pico BS).

C. Matching model parameters

Fig. 2 and Fig. 3 illustrate and compare coverage probabilities P_c obtained using the 3GPP simulated model and the stochastic geometry model for 1-tier network deployment: either only macro or only pico BS, respectively. Here, we used least square error method to determine the exact value of the path loss parameter α which best fits the real 3GPP model. The figures illustrate that $\alpha = 2.5$ and $\alpha = 4$ represent the best fit to the real 3GPP model for only macro and only pico 1-tier eNB deployment [10].

Fig. 4 presents compare coverage probabilities P_c which are obtained using the 3GPP model and the stochastic geometry model for 2-tier networks (both macro and pico BS) in the same manner as explained above. The figure presents that $\alpha = 3.5$ represents the best fit to the real 3GPP model for macro and pico BS 2-tier eNB deployment [10].

IV. eMBMS Rate vs Coverage Performance

After we have calibrated stochastic geometry expressions to the simulated 3GPP model, in this section, we provide

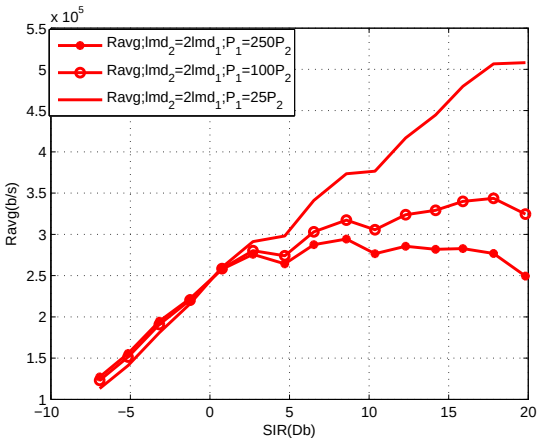

Fig. 5. Average data rate for power ratio (P_1/P_2=25;100;250) and density ratio (λ_1/λ_2=2).

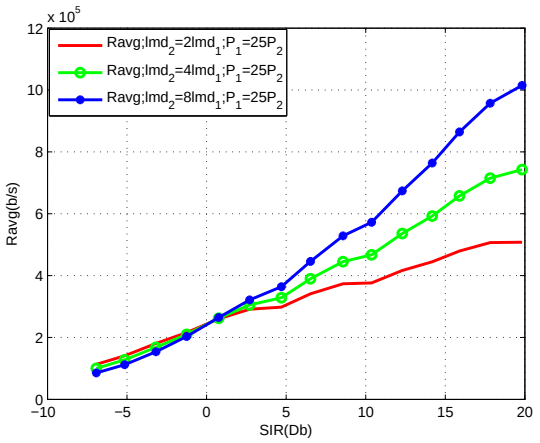

Fig. 6. Average data rate for power ratio (P_1/P_2=25) and density ratio (λ_1/λ_2=2;4;8).

results on achievable rates for eMBMS-based video multicast service delivered over LTE-A HetNets modelled as the two-tier cellular systems. We use the results from III, i.e., we apply stochastic geometry based analysis to obtain coverage probabilities for different power and density ratios among the two tiers of base stations.

Regarding the achievable data rates at the UEs, we assume the following model. The PHY layer of the serving eNB may be configured to a specific MC scheme corresponding to channel quality (CQI) values 0–15 (see Sec. II-B). If the eNB delivers eMBMS service using an MC scheme corresponding to the CQI value i, we assume that all the UEs whose SINR exceeds the threshold SINR(i) for reception of the MC scheme i (i.e., all the UEs that are in coverage of MC scheme i), will be able to receive reliably this service. The average data rate achievable at the UE which is in coverage of MC i is:

$$R_i = \frac{TBS(i) \cdot N_{RBP}}{TTI}(1 - BLER(i)), \qquad (5)$$

where $TBS(i)$, $BLER(i)$ (see II-B) is the PHY TB information capacity (in bits) and the average BLER of the i-th MC scheme (e.g., usually, $BLER(i)$ is fixed to approx. 10% PHY TB loss rate for any MC scheme [14]).

Finally, the average data rate $R_{avg}(i)$ of the PHY TB data delivery across an LTE-A HetNets is obtained by weighting the data rate of covered UEs with the coverage probability for each of available MC schemes:

$$R_{avg}(d) = R_i \cdot P_c(i), \qquad (6)$$

where R_i, $P_c(i)$ are the data rate (equation 5) and the coverage probability UE when the MC scheme corresponding to the CQI value i is selected.

The question we would like to answer is how to optimally select the PHY transmission scheme, i.e., which of the available MC configurations to use in order to maximally exploit eMBMS service in two-tier system configuration. Note that if we increase the MC scheme applied in service delivery, we are increasing the rate (and thus the quality of service/experience) of the users that receive the service, but we decrease the coverage, so there is an evident design trade off. We provide the average system throughput for different system configurations (power and density ratios in two-tier setup for different MC schemes) by multiplying the rate delivered to covered users with the coverage probability (i.e., the fraction of the total area being covered). We discuss the obtained average results in terms of main system parameters: power ratio (P_1/P_2 = 25; 100; 250), density ratio (λ_1/λ_2 = 2; 4; 8) and the applied MC scheme. The above parameters roughly correspond to 2-tier micro and pico, and 2-tier macro and femto base station deployments.

A. Numerical Results

Figure 5 shows the results obtained for the scenario where the density ratio among the base station tiers is fixed, while the power ratio among the tiers is varied. We consider $\lambda_1/\lambda_2 = 2$ which corresponds to sparse deployment of small cells (only two small cells per macro cell on average). We note that for large power ratio $P_1/P_2 = 250$ corresponding to macro-to-femto power ratio, the increase of the MC scheme does not result in increasing of the average rate in network, while the coverage is decreasing. Thus there exists an MC scheme (in Fig. 5, this is approximately CQI 6 at SIR=3dB) such that by further increase of the MC index, the average user rate does only marginally increase, while coverage is dramatically decreasing. For lower power ratio $P_1/P_2 = 25$ corresponding to macro-to-micro power ratio, the average rate increase with the increase of the MC scheme is nearly linear. This is due to the fact that, with the increase of the applied MC scheme, the user data rates in covered areas increase considerably faster than the coverage probability P_c is decreasing. This results in apparent anomaly situation where the average cell rate is obtained in a configuration where a very high throughput is offered to users in a very small coverage area. In this case, the average data rate metric as defined in (6) is clearly not the best criterion because it takes into account the average rate but not the general state of the network.

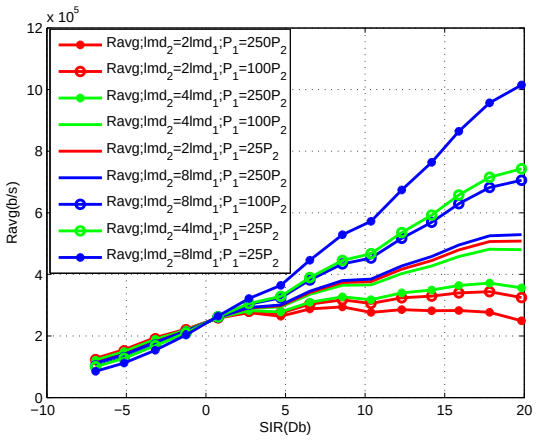

Fig. 7. Average data rate for all combination power ratio (P_1/P_2=25;100;250) and density ratio (λ_1/λ_2=2;4;8).

Figure 6 illustrates the results obtained for scenario where the power ratio P_1/P_2 is fixed, while the density ratio is changed. In particular, we apply $P_1/P_2 = 25$ corresponding to macro-to-micro scenario. Increasing the density ratio λ_1/λ_2, the average rate demonstrates linear increase. However, the coverage probability also improves with increased λ_1/λ_2. Thus although by increasing MC scheme, we in general decrease the coverage area, this can be to some extent compensated by the increase in λ_1/λ_2.

Figure 7 demonstrates that the average rate for various pairs of power and density ratios generally favours the increase of the MC scheme. However, in the extension of this study, we will introduce additional metrics that would aim at establishing better balance between the average rate and coverage area achieved within multi-tier scenario.

V. Conclusions

In this paper, we analysed average achievable rates for recently proposed 3GPP strategies for video multicasting and broadcasting service delivery over LTE/LTE-A HetNets. We presented a simple analytical approach for average service rate calculation based on stochastic geometry analysis and consider the resulting rates under constraints of coverage probability requirements. The average service rate results are compared and a number of trade-off parameters has been established such as power ratio (P_1/P_2), density ratio (λ_1/λ_2) and physical layer modulation and coding scheme applied. As a demonstration, achievable rates are evaluated for the SC-eMBMS configurations in the two-tier cellular systems.

References

[1] Cisco Visual Networking Index, http://www.cisco.com/en/US/netsol/ /ns827/networking solutions sub solution.html

[2] A. Ghosh, R. Ratasuk, B. Mondal, N. Mangalvedhe, and T. Thomas, LTE-Advanced: next-generation wireless broadband technology, IEEE Wireless Communications, vol.17, No. 3, pp. 1022, June 2010.

[3] ETSI TS 26.346 v10.1.0 (Rel. 10), UMTS-Multimedia Broadcast/Multicast Service (MBMS); Protocols and Codecs, October 2011.

[4] M. Gruber and D. Zeler, Multimedia Broadcast Multicast Service: New Transmission Scheme and Related Challenges, *IEEE Comm. Magazine,* Vol. 49, No. 12, pp. 176-181, Dec. 2011.

[5] J. Xu, J. Zhang, and J. Andrews, On the accuracy of the Wyner model in cellular networks, IEEE Trans. Wireless Commun., vol. 10, no. 9, pp. 30983109, Sept. 2011.

[6] H. S. Dhillon, R. K. Ganti, F. Baccelli, J. G. Andrews, Modeling and analysis of K-tier downlink heterogeneous cellular networks. Selected Areas in Communications, IEEE Journal on, 30(3), 550-560, April 2012.

[7] H. S. Jo, Y. J. Sang, P. Xia, J. G. Andrews, Heterogeneous cellular networks with flexible cell association: A comprehensive downlink SINR analysis. Wireless Communications, IEEE Transactions on, 11(10), 3484-3495, August 2012.

[8] O. Oyman, J. Foerster, T. Y-J. Tcha, S-C. Lee, "Towards Enhanced Mobile Video Services over WiMAX and LTE," *IEEE Comm. Magazine,* Vol. 48, No. 8, pp. 68-76, Aug. 2010.

[9] M. Sawahashi, Y. Kishiyama, A. Morimoto, D. Nishikawa, M. Tanno: Coordinated Multipoint Transmission/Reception Techniques for LTE-Advanced, IEEE Wireless Communications, Vol.17, No.3, pp.2634, June 2010.

[10] 3GPP TR 36.814 V2.0.0, Further Advancements for E-UTRA Physical Layer Aspects, March 2010.

[11] H. Holma and A. Toskala, LTE for UMTS : Evolution to LTE-Advanced, Second Edition, Wiley, 2011.

[12] C. Khirallah, D. Vukobratovic, and J. Thompson: Bandwidth and Energy Efficiency of Video Broadcasting Services over LTE/LTE-A, IEEE WCNC 2013, Shanghai, China, April 2013.

[13] ETSI TS 136 213 V10.7.0 (Rel. 10), LTE; Evolved Universal Terrestrial Radio Access (E-UTRA); Physical layer procedures, October 2012.

[14] A. Larmo, M. Lindstrom, M. Meyer, G. Pelletier, J. Torsner, H. Wiemann: The LTE Link-Layer Design, *IEEE Comms. Mag.*, Vol. 47, No. 4, pp: 52-59, April 2009.

[15] H. S. Dhillon, R. K. Ganti, F. Baccelli, and J. G. Andrews: Modeling and analysis of K-tier downlink heterogeneous cellular networks, Selected Areas in Communications, IEEE Journal on, 30(3), 550-560, December 2012.

[16] J. G. Andrews, F. Baccelli, and R. K. Ganti: A tractable approach to coverage and rate in cellular networks, IEEE Trans. on Communications, vol. 59, no. 11, pp. 3122 3134, Nov. 2011.

[17] 3GPP TR 36.913 V8.0.1 (Release 8), Requirements for further advancements for E-UTRA, March 2009.